

Cannabinoid CB2/CB1 Selectivity. Receptor Modeling and Automated Docking Analysis

Tiziano Tuccinardi, Pier Luigi Ferrarini, Clementina Manera, Gabriella Ortore, Giuseppe Saccomanni, and Adriano Martinelli*

Dipartimento di Scienze Farmaceutiche, Università di Pisa, via Bonanno 6, 56126 Pisa, Italy

Received September 5, 2005

Three-dimensional models of the CB1 and CB2 cannabinoid receptors were constructed by means of a molecular modeling procedure, using the X-ray structure of bovine rhodopsin as the initial template, and taking into account the available site-directed mutagenesis data. The cannabinoid system was studied by means of docking techniques. An analysis of the interaction of WIN55212-2 with both receptors showed that CB2/CB1 selectivity is mainly determined by the interaction in the CB2 with the nonconserved residues S3.31 and F5.46, whose importance was suggested by site-directed mutagenesis data. We also carried out an automated docking of several ligands into the CB2 model, using the AUTODOCK 3.0 program; the good correlation obtained between the estimated free energy binding and the experimental binding data confirmed our binding hypothesis and the reliability of the model.

Introduction

It has been about 41 years since Gaoni and Mechoulam identified Δ^9 -tetrahydrocannabinol (THC) as the principal psychoactive molecule present in cannabis.^{1,2} The pharmacological effects of cannabinoids are mediated through at least two receptors, termed CB1 and CB2, although recently, a lot of evidence has been reported about the detection in mouse brain of a third cannabinoid receptor subtype.³

Regarding their distribution and functionality, CB1 receptors are predominantly located in the central nervous system, and they are probably responsible for most of the overt pharmacological effects of cannabinoids.^{4–7} The CB2 receptor is found in peripheral tissues, such as spleen, tonsils, and immunocytes.⁸ This subtype is of particular interest, since it has been identified as a potential target for therapeutic immune treatment, due to its involvement in signal transduction processes in the immune system. Furthermore, a synthetic analogue of THC has recently proved to have significant antiinflammatory and antitumor effects without any psychoactive effects, and it has been determined that its antineoplastic effect was mediated primarily through actions on CB2 receptors. For all these reasons, at present, research and development of new potent and selective ligands for CB2 is still of great importance.⁹

Both CB1 and CB2 are seven-transmembrane (TM) receptors that belong to the rhodopsin-like family Class A of G protein-coupled receptors (GPCRs) and control a wide variety of multiple intracellular signal transduction pathways. CB1 and CB2 agonists inhibit adenylyl cyclase by activation of a pertussis toxin-sensitive G-protein;¹⁰ moreover CB1 activation inhibits the calcium channels and activates inwardly rectifying potassium channels.¹¹

How do GPCRs change their conformations, in response to agonist binding, to activate the associated G-proteins? There are two main hypotheses to account for ligand-mediated G-protein activation, *conformational selection model*¹² and *ligand induction model*.¹³ According to the *conformational selection model*, there are two conformations of the receptor, the inactive (R) and the active (R*) one; the agonist preferentially binds the receptor in the R* conformation, thus increasing the duration of the period in which the receptor remains in the active state.

The *ligand induction model* predicts that transition between the R and R* state is extremely rare in the absence of the agonist, and the free energy of the agonist binding to R is used to facilitate (or induce) the transition to R*.

Bovine rhodopsin, crystallized by Palczewsky et al.,¹⁴ provided the first direct visualization of the seven-transmembrane helices of a G-protein-coupled receptor in the inactive state. Regarding the activated state, spectroscopic techniques on purified receptor preparations permitted the first direct insight into structural changes that occur during receptor activation, suggesting the conformational differences between the inactive and active states.¹³

A knowledge of the 3D structure of cannabinoid receptors could be of great help in the task of understanding their function and in the rational design of specific ligands. For this purpose, many biochemical, pharmacological, and computational studies have been carried out on cannabinoid receptors.

Cannabinoid receptor agonists can be divided into four structurally distinct classes of compounds. These include classic cannabinoids (like Δ^9 -THC), nonclassical cannabinoids, represented by CP55940, aminoalkylindoles, such as WIN55212-2, and endogenous cannabinoids such as arachidonylethanolamide, also called anandamide (AEA).¹¹

Aminoalkylindoles derivatives are structurally dissimilar from the other classes, and as site-direct mutagenesis has revealed that the set of amino acids important for their binding differs significantly from those of the other classes of ligands, the binding site of this type of ligand is probably different from the others.¹⁵

Regarding in the CB1 receptor more specifically, mutation studies have reported that a K3.28(192)A mutation results in a greater loss in affinity for AEA and CP55940, while the WIN55212-2 affinity remains unchanged.¹⁶ In the other case, the mutation of F3.36(191)A, W5.43(279)A, and W6.48(356)A in the CB1 receptor determined a loss of affinity only for WIN55212-2, whereas the AEA and CP55940 affinity was unaffected.¹⁷ Regarding the CB2 receptor, Song and co-workers reported that the mutation of F5.46(197)V determined a 14-fold decrease in CB2 affinity for WIN55212-2, while the CP55940 and AEA affinity was unchanged.¹⁸

In the present study, we constructed and refined a three-dimensional model of the CB1 and CB2 receptors in their activated forms. Furthermore, we analyzed the docking of

* To whom correspondence should be addressed. E-mail: marti@farm.unipi.it; Fax: ++39 050 2219605; phone: ++39 050 2219556.

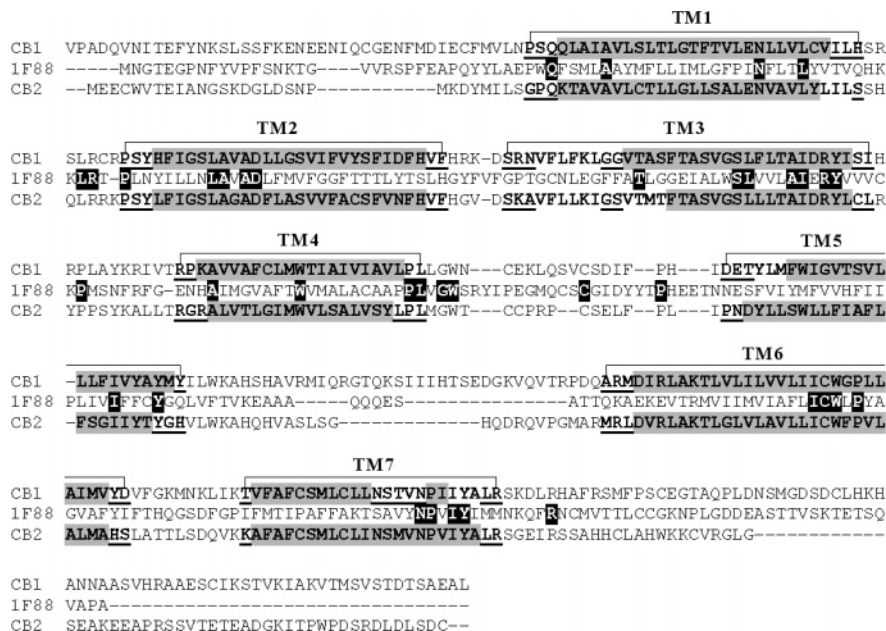


Figure 1. Alignment of the cannabinoid receptors and bovine rhodopsin (1F88) amino acid sequences. The identical residues are highlighted in black, while the α helix and β sheet prediction carry out by Psipred is respectively marked in gray and underlined.

WIN55212-2 in both receptor models, with the aim of finding the reasons for its selectivity toward the CB2 receptor. Finally, the CB2 receptor model thus constructed was used for an automated docking approach on several selective CB2 ligands by means of AUTODOCK 3.0.¹⁹

Results and Discussion

Molecular Modeling. Models of the CB1 and CB2 receptors were generated using the bovine rhodopsin structure determined at 2.8 Å as a template.¹⁴ The length of the transmembrane helices of the two receptors was defined by aligning the rhodopsin primary sequence with both receptor sequences using CLUSTAL W²⁰ and verifying the probable presence of the α -helix by means of the Psipred program (see Figure 1).^{21,22} Following the suggestion of Salo et al.,²³ we omitted the highly conserved proline residue P5.50(215) of rhodopsin, considering the presence of a gap in that position.

It is well-known that rhodopsin was crystallized in its inactive state, and therefore the CB models obtained with the procedure described above represent an inactivated state; according to the activation hypothesis, this state is not suitable for studying the binding of agonists, and the receptor models should be built in their active state.

The activation of the GPC receptors seems to be determined by a different rearrangement of TM3 and TM6, since the disruption of interaction between these two helices produces constitutive receptor activation, and in particular, the extent of constitutive activation is closely correlated with the extent of conformational rearrangement in TM6.²⁴ Computational and experimental studies have indicated that conformational switches can be generated in the TM helices as a result of the formation of flexible molecular hinges by a residue of proline.²⁵

During activation in the β_2 adrenergic receptor, P6.50(288) permits the movement of the intracellular end of TM6 away from TM3 and upward toward the lipid bilayer, suggesting that probably the crucial movements for activation involve flexibility about the hinge formed by the highly conserved proline in TM6 (P6.50).²⁶ Conformational memories calculations of TM6 in the β_2 adrenergic receptor, combined with mutation and SCAM studies, suggested the presence of a rotamer toggle switch able

to modulate the TM6 proline kink; according to this hypothesis C6.47(285)_trans/W6.48(286)_gauche+/F6.52(290)_gauche+ represents the inactive form of the β_2 adrenergic receptor, while C6.47_gauche+/W6.48_trans/F6.52_trans represents the active state.²⁷

Regarding the activation of CB receptors, Singh and co-workers suggested that W6.48(356)/F3.36(200) interaction may act as the toggle switch for CB1 activation, with W6.48_gauche+/F3.36_trans representing the inactive and W6.48_trans/F3.36_gauche+ the CB1 active form.²⁸ Following the indications of these studies, therefore, to analyze the agonist binding interaction, we modified the inactive template of our CB1 and CB2 receptors by rotating TM3 and TM6 in a counterclockwise direction (extracellular point of view) and straightening TM6, using P6.50 as a flexible hinge; finally, we adjusted the conformation of the χ_1 rotamer of W6.48 and F3.36: trans the former and gauche+ the latter. The receptor models thus obtained were optimized through 400 ps of molecular dynamics (MD), in accordance with the procedure described in the Experimental Section.

The backbone conformation was evaluated by inspection of the Psi/Phi Ramachandran plot obtained from PROCHECK analysis.²⁹ As shown in the Ramachandran plots of Figure 2, the distribution of the Psi/Phi angles of both models are within the allowed regions and no residue has a disallowed conformation.

Docking of WIN55212-2. The models obtained with these calculations were complexed with a high affinity ligand, and the complexes were optimized. WIN55212-2 was chosen for this purpose, since it is commonly used in binding experiments and because it shows a high activity in both receptors, in particular CB2 (see Table 3). It was docked bearing in mind the known mutagenesis data.

In the CB1 receptor F3.36(200), W5.43(279), and W6.48(356) might be important for WIN55212-2 binding,¹⁷ whereas CB2 mutagenesis studies suggest the importance of S3.31(112)³⁰ and F5.46(197)¹⁸ in this subtype. To consider these interactions, we inserted the ligand with the morpholinic group positioned between TM3 and TM4, while the naphthyl substituent was directed toward the central core of TM5 and TM6. In this

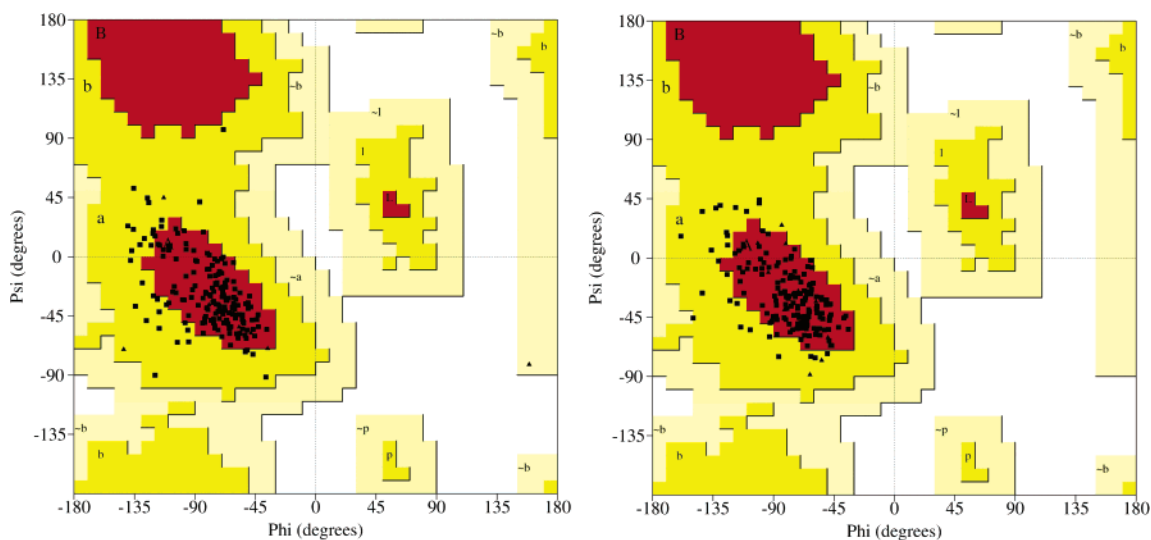


Figure 2. Ramachandran plot of the CB1 (on the left) and CB2 (on the right) receptor. The most favored regions are colored red, additional allowed, generously allowed, and disallowed regions are indicated as yellow, light yellow, and white fields, respectively.

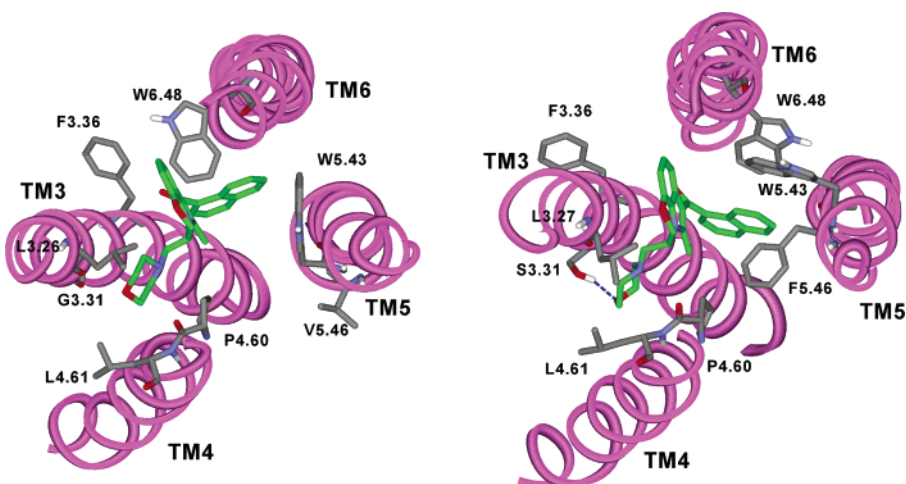


Figure 3. WIN55212-2 docked into the CB1 (left) and CB2 (right) receptors (extracellular point of view).

Table 1. Principal WIN55212-2–Receptor Interaction in CB1 and CB2^a

	WIN55212-2					
	interaction with CB1 (distance in Å)			interaction with CB2 (distance in Å)		
	naphthyl	indole	morpholinic	naphthyl	indole	morpholinic
L3.26	—	5.43	3.52	—	4.21	—
F3.27/L3.27	—	—	6.25	—	3.50	4.06
G3.30/S3.31	—	—	3.81	—	5.68	3.20
F3.36	4.94	5.70	—	—	—	—
P4.60	—	4.01	3.72	—	3.69	3.59
L4.61	—	—	3.90	—	—	3.78
W5.43	4.37	6.70	—	3.54	6.20	—
V5.46/F5.46	—	—	—	4.08	—	—
W6.48	—	5.05	—	5.90	—	—

^a Distances exceeding 7 Å are not reported but indicated as —.

manner, the lipophilic core of the ligand was able to interact with W5.43 and W6.48, and in the CB2 receptor the naphthyl ring could interact with F5.46(197) and the morpholinic group with S3.31(112).

The two complexes were then submitted to 400 ps of MD (see Experimental Section for details), and Figure 3 shows the docking of the ligand in the two receptors. In the CB1R, the binding site is characterized by a lipophilic pocket delimited by F3.36(200), W5.43(279) and W6.48(356), which principally interact through aromatic stacking with the naphthyl and indole ring system (for distance analysis, see Table 1), while the

morpholinic group is positioned in a secondary lipophilic pocket formed by L3.26(190), P4.60(251) and L4.61(252). The CB2 binding site is similar to the CB1 one, with a primary lipophilic pocket delimited by F3.36(117), W5.43(194), W6.48(258), but the WIN55212-2 orientation is slightly different. In the CB2 site, the ligand veers away from F3.36(117), since it feels the effect of a strong interaction with F5.46(197), which is a nonconserved residue (V5.46(282) in the CB1) capable of stabilizing the naphthyl ring. Regarding the secondary lipophilic pocket in which the morpholinic group is positioned, the substituent interacts with L3.27(108), P4.60(168), and L4.61(169),

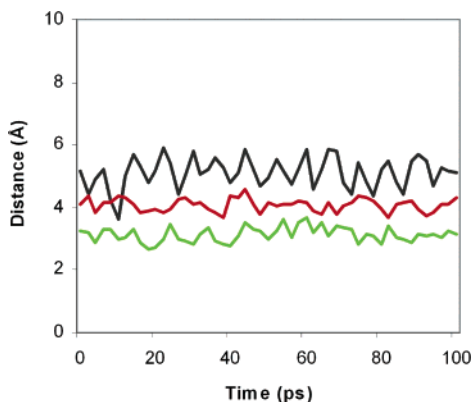


Figure 4. Distances of the main interaction between WIN55212-2 and the CB2 receptor during the last 100 ps of MD simulation. In black, distances between the naphthyl ring of the ligand and the centroid of the aromatic nucleus of F5.46(197), in red, distances between the centroid of the naphthyl ring and the indole of W5.43(194), in green, distances between the O of the morpholinic ring and the OH of the S3.31(112). The distances were updated every 2 ps.

and the nonconserved S3.31(112) (G3.31(195) in the CB1R) forms a hydrogen bond with the oxygen atom of the morpholinic group. As can be seen in Figure 4, the main interactions of WIN55212-2 with the CB2 receptor were stable: the hydrogen bond with S3.31(112), the aromatic stacking, and the π - π interaction of the naphthyl ring with F5.46(197) and W5.43(194), respectively, were maintained during all the last 100 ps of MD.

To validate our hypothesis and to characterize the structural differences of the two binding sites, we examined the molecular interaction fields (MIFs) obtained by means of the GRID program³¹ for 10 different probes (see Table 2). An analysis using C1= and C3 probes showed the presence in both receptors of a large lipophilic pocket corresponding to the space occupied by the naphthyl and indole ring of WIN55212-2, and a secondary one corresponding to the morpholinic position. Moreover, the OC2 probe showed the presence in the CB2 binding site of a favorable interaction area in the space occupied by the morpholinic group (see Figure 5). Thus, the observation of the two binding sites and an analysis using different probes encouraged us to carry on a further development of these models.

Docking of AEA. To further test the validity of the models, we docked into both receptors the most well-known endogenous

Table 2. Overview of GRID Probes Used in This Study

name	chemical group
DRY	hydrophobic probe
C1=	sp ² CH aromatic or vinyl
C3	methyl CH ₃ group
OC2	ether oxygen
OH	phenol or carboxy OH
N:	sp ³ N with lone pair
CL	organic chlorine atom
O	sp ² carbonyl oxygen
O1	alkyl hydroxyl OH group
ArCONHR	aromatic cis or trans amide

ligand AEA, which has a completely different structure with respect to WIN55212-2, through an automated docking procedure (see Experimental Section for details).

In CB1 AEA adopts an U-shaped molecular conformation and it is placed among TM2–3–6–7 with the aliphatic chain directed toward the intracellular side of the receptor. The amide oxygen atom of the ligand interacts with K3.28(193), in agreement with site-directed mutagenesis studies,¹⁶ and the hydroxy group forms an H bond with S7.39(383). The residues that delimited the AEA binding pocket are principally hydrophobic, including F2.57(170), F3.25(189), L3.29(193), V3.32(196), F3.36(200), and F7.35(379), in agreement with the CB1 model proposed by McAllister et al.¹⁷ Anyway, differently from this model, in our study F2.57(170) interacts with the aliphatic chain of AEA through a C–H \cdots π interaction, whereas F3.25(189) has an interaction with the amide oxygen atom.

In the CB2 receptor AEA does not interact with K3.28(109), but it forms a H-bond with S3.31(112) through the amide oxygen atom, and this is in agreement with mutagenesis studies.³⁰ Moreover, the hydroxy group interacts with the oxygen backbone of L3.27(108). The CB2–AEA binding is included among TM3–4–5–6, as for WIN55212-2, and the AEA aliphatic chain interacts principally with W5.43(194) and W6.48(258). The AEA docking results seem to support the validity of these CB1 and CB2 models since they are in good agreement with the main mutagenesis data available for this ligand.

Automated Docking. In order to investigate the characteristics of the CB2 model and also its predictivity, we chose from relevant literature 96 ligands (see Table 3) that probably interact in the WIN55212-2 binding site, and using the AUTODOCK 3.0 program¹⁹ we docked these compounds into the CB2 model.

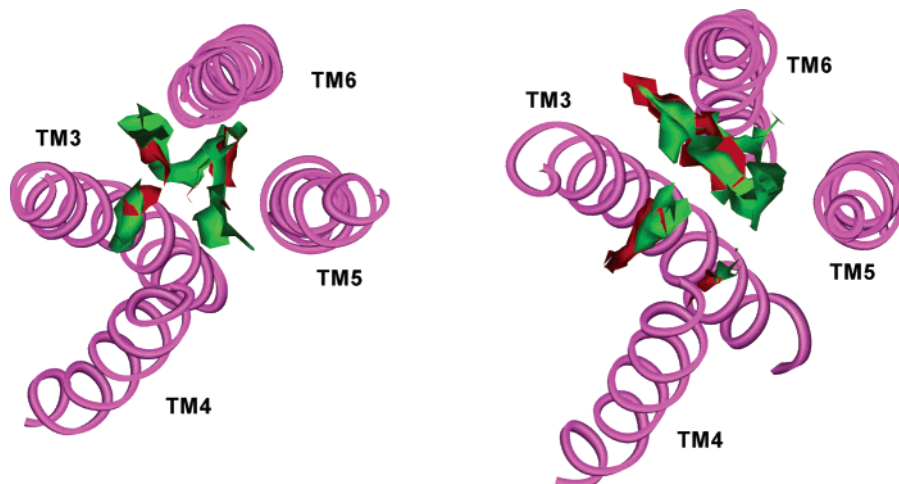
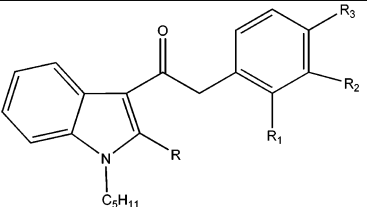


Figure 5. GRID analysis using the C1= (green surface) and OC2 (red surface) probes into the CB1 (left) and CB2 (right) receptors. The C1 probe shows the presence in both receptors of a large lipophilic pocket and a small secondary one, while the OC2 probe shows the presence in the CB2 receptor of a favorable interaction area in the secondary lipophilic pocket.

Table 4. Structure and Binding Data of the Ligands Used as Test Set^a


Compd	R	R ₁	R ₂	R ₃	G exp	G pred	Cluster
JWH-167 ³⁸	H	H	H	H	-9.27	-8.52	Ener.
JWH-205 ³⁸	CH ₃	H	H	H	-9.20	-8.45	Ener.
JWH-251 ³⁸	H	CH ₃	H	H	-9.32	-8.94	Ener.
JWH-252 ³⁸	CH ₃	CH ₃	H	H	-9.93	-9.75	Ener.
JWH-208 ³⁸	H	H	H	CH ₃	-8.51	-8.15	Ener.
JWH-209 ³⁸	CH ₃	H	H	CH ₃	-8.00	-8.22	Ener.
JWH-250 ³⁸	H	OCH ₃	H	H	-10.20	-9.38	Ener.
JWH-306 ³⁸	CH ₃	OCH ₃	H	H	-9.66	-10.46	Ener.
JWH-302 ³⁸	H	H	OCH ₃	H	-9.61	-8.54	Ener.
JWH-253 ³⁸	CH ₃	H	OCH ₃	H	-9.65	-9.31	Ener.
JWH-201 ³⁸	H	H	H	OCH ₃	-8.66	-7.78	Ener.
JWH-202 ³⁸	CH ₃	H	H	OCH ₃	-8.44	-8.68	Ener.
JWH-311 ³⁸	H	F	H	H	-10.10	-9.52	Ener.
JWH-314 ³⁸	CH ₃	F	H	H	-9.71	-9.10	Ener.
JWH-312 ³⁸	H	H	F	H	-9.60	-8.22	Ener.
JWH-315 ³⁸	CH ₃	H	F	H	-9.19	-9.24	Ener.
JWH-313 ³⁸	H	H	H	F	-8.78	-8.15	Ener.
JWH-316 ³⁸	CH ₃	H	H	F	-8.33	-8.66	Ener.
JWH-203 ³⁸	H	Cl	H	H	-11.12	-10.03	Ener.
JWH-204 ³⁸	CH ₃	Cl	H	H	-10.36	-9.63	Ener.
JWH-237 ³⁸	H	H	Cl	H	-9.51	-9.01	Ener.
JWH-303 ³⁸	CH ₃	H	Cl	H	-9.35	-9.93	Ener.
JWH-206 ³⁸	H	H	H	Cl	-8.59	-7.59	Ener.
JWH-207 ³⁸	CH ₃	H	H	Cl	-7.40	-7.68	Ener.
JWH-249 ³⁸	H	Br	H	H	-10.50	-10.37	Ener.
JWH-305 ³⁸	CH ₃	Br	H	H	-10.28	-10.03	Ener.
JWH-248 ³⁸	H	H	H	Br	-8.43	-7.64	Ener.
JWH-304 ³⁸	CH ₃	H	H	Br	-7.60	-7.66	Ener.
SDEP	0.66						

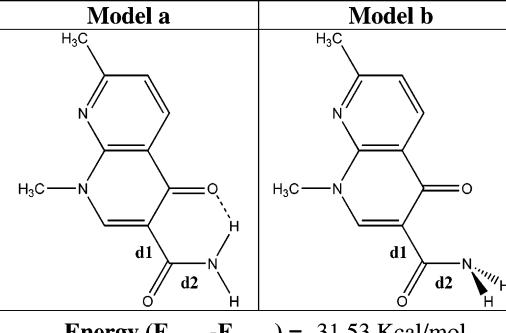
^a In the last column is indicated which cluster was used in the automated docking. (Ener. = the cluster with the best average of estimated free energy, Pop. = the best populated cluster, “—” means the considered cluster does not belong to none of these two classes). “G sper” and “G pred” indicate, respectively, the experimental and predicted binding free energy (kcal/mol). In the last row is reported the SDEP value.

On the basis of their central nucleus and substituents, they can be divided into two classes, indole and naphthyridine derivatives.

Concerning the indole derivatives, GTP γ S assays indicated that **JWH-151** is a full agonist at CB2, whereas **JWH-120** and **JWH-267** are partial agonists;³² as for the naphthyridine derivatives, our studies concerning the modulation of mast cell activation³³ highlight that compound **3g** is a full agonist.³⁴ For these reasons we consider it more reasonable to dock all the ligands tested into the activated form of the CB2 receptor.

The chosen parametrization of AUTODOCK (see Experimental Section) was tested for its ability to reproduce the binding geometry of WIN55212-2 obtained by means of the molecular dynamics procedure. AUTODOCK easily found the binding geometry corresponding to the one obtained by manual docking, as the rms deviation between the lowest energy docked conformation and the WIN55212-2 manually docked one was 0.62 Å (rms evaluated over all the heavy atoms of the ligand).

Analysis of Naphthyridine Derivatives. These compounds can form an intramolecular H bond between the carbonylic oxygen atom and the amidic NH (see Table 5). Our studies suggested that this interaction had a high strength, about 30 kcal/mol (see Experimental Section for details), and consequently this H bond was considered to be maintained also during interaction in the binding site. For this reason, during the AUTODOCK protocol, we blocked the torsions involved in this intramolecular bond (torsions **d1** and **d2** in Table 5), to prevent the loss of this interaction.

Table 5. Energy Difference between the Two Optimized Models


Energy (E_{model a} - E_{model b}) = -31.53 Kcal/mol

Figure 6A shows the docking of **3a** into the CB2 binding site. The ligand position is similar to that of WIN55212-2: **3a** gives H bonds with S3.31(112) through the morpholino substituent, and there is a lipophilic interaction between the cyclohexyl group and W5.43(194) and F5.46(197), in agreement with the mutagenesis data and our binding hypothesis. Regarding the naphthyridine ring, it is stabilized by lipophilic interaction with L3.26(107), I3.29(110), M6.55(265), and L6.59(269).

Compound **6a** is 20-fold more potent than **3a** and differs only in the R group, because the ethylmorpholino group is substituted by the *p*-F-benzyl moiety. As shown in Figure 6B, the lowest energy docked conformation of compound **6a** has a binding position very similar to the one shown by **3a** (the rms between the heavy atom positions of the naphthyridine rings of the two ligands in the CB2 binding site is 0.58 Å). As for **3a**, the cyclohexyl group of compound **6a** interacts with W5.43(194) and F5.46(197) while the R substituent forms an H bond with S3.31(112) (with the fluorine atom). Moreover, the aromatic ring of this substituent is stabilized by the secondary lipophilic pocket formed by L3.27(108), P4.60(168), and L4.61(169), and this could be the reason for the higher affinity shown by this ligand.

The presence of a benzyl substituent in R₁ determines a decrease in the affinity. For example, compound **6e** differs from **6a** only in the presence of the R₁ benzyl instead of the cyclohexyl group and shows a 10-fold lower affinity for the CB2 receptor.

The superimposition of the binding site of **6e** on that of **6a**, shows that in the docking of **6e**, the presence of an R₁ rigid substituent like benzyl causes a translation of the naphthyridine ring toward the extracellular side of the receptor (the rms between the heavy atoms of **6e** and **6a** naphthyridine rings is 2.12 Å), determining worse interactions with the residues that stabilize the naphthyridine ring (see Figure 6C), with the consequent decrease in affinity.

Analysis of Indole Derivatives. All the compounds that present a 3-(1-naphthoyl)indole as their central nucleus show a binding position very similar to the one observed for WIN55212-2. The docking of compound **JWH-007**, which is 10-fold less potent than WIN55212-2, shows that the naphthyl ring is stabilized by W5.43(194), F5.46(197), and M6.55(265), while the indole ring interacts with L3.26(107), I3.29(110), and L6.59(269). The R pentyl substituent is inserted into the secondary lipophilic pocket formed by L3.27(108), P4.60(168), and L4.61(169), but of course it is not able to form the H bond with S3.31(112), and this could be one of the reasons for the lower affinity of this ligand, compared with that of the WIN55212-2 affinity (see Figure 7A).

The compounds (**1–17**) bearing the morpholinic ring linked to the C³ position of the indole system and the aromatic group

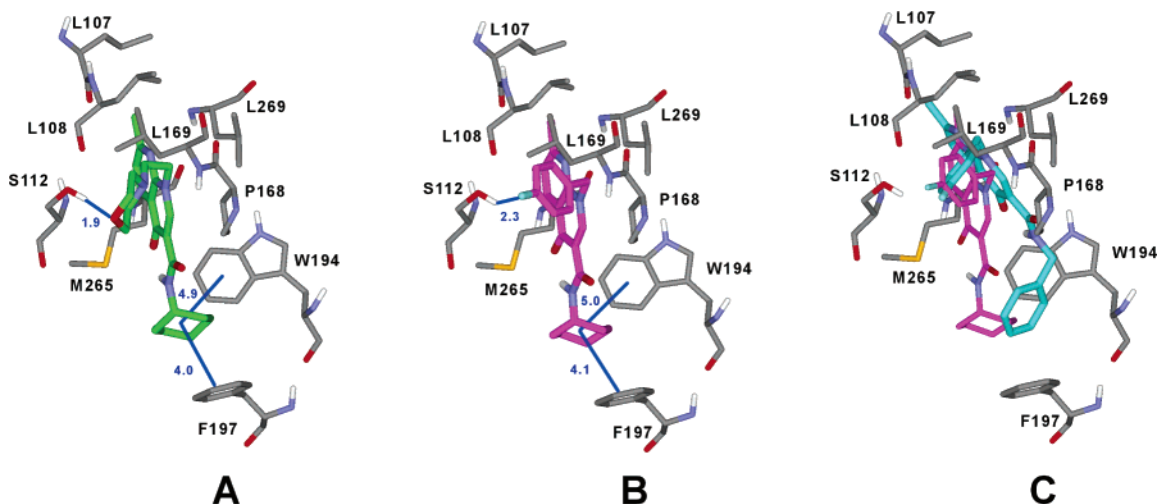


Figure 6. Docking of **3a** (A), **6a** (B), and superimposition (C) of ligands **6a** and **6e** (respectively colored magenta and sky blue) in the CB2 binding site. The main interatomic distances are reported in blue, all distances are in angstroms.

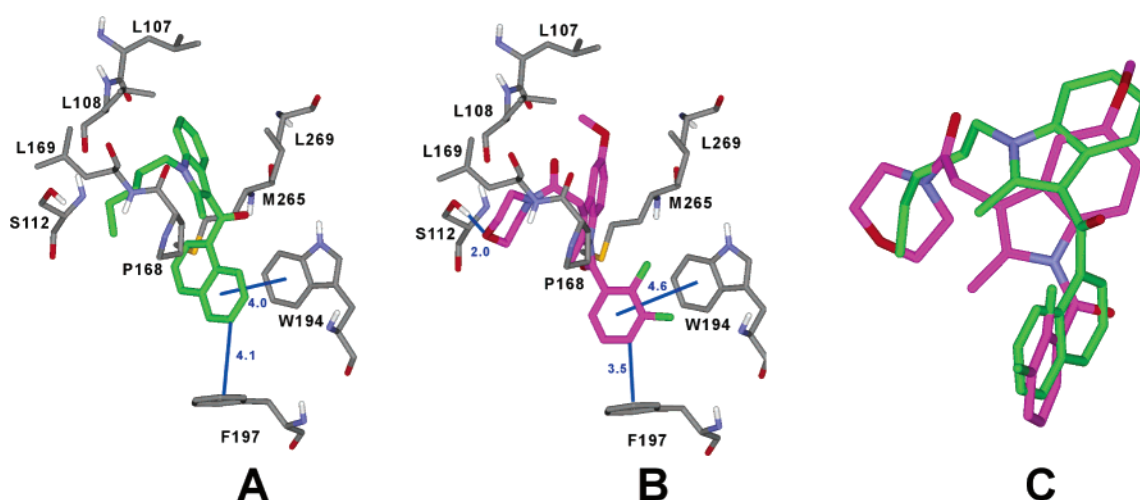


Figure 7. Docking of **JWH-007** (A) and **9** (B) into the CB2 binding site, and superimposition of the two ligands (C) showing the opposite disposition of the indole ring, with the nitrogen pointing toward the intracellular side of the receptor for compound **9** and toward the extracellular side for **JWH-007**.

linked to the N¹ position (in an opposite manner compared with WIN55212-2, which presents the morpholinic substituent linked to N¹ and the 1-naphthoyl group in the C³ position), show a different placement of the indole ring in the CB2 binding site, compared with the indole position of the 3-(1-naphthoyl)indole analyzed.

The docking of compound **9**, which presents these structural characteristics, shows that the 3-acetylmorpholine moiety is inserted into the secondary lipophilic pocket and forms the H bond with S3.31(112), while the N¹-2,3-dichlorobenzoyl substituent interacts with W5.43(194), F5.46(197) in the same manner as the naphthyl group of the 3-(1-naphthoyl)indole compounds (see Figure 7B). Comparing the position of **JWH-007** with that of this ligand, we observe that the aromatic and morpholinic groups have the same disposition, but for this reason, unlike from **JWH-007**, the indole ring of compound **9** is upset, with the nitrogen directed toward the intracellular side of the receptor (see Figure 7C). These observations might suggest that the nitrogen of the indole system should not be important for the interaction, and that the role of the whole indolic system could be only that of an aromatic core able to place the substituents in the right disposition in the CB2 receptor binding site.

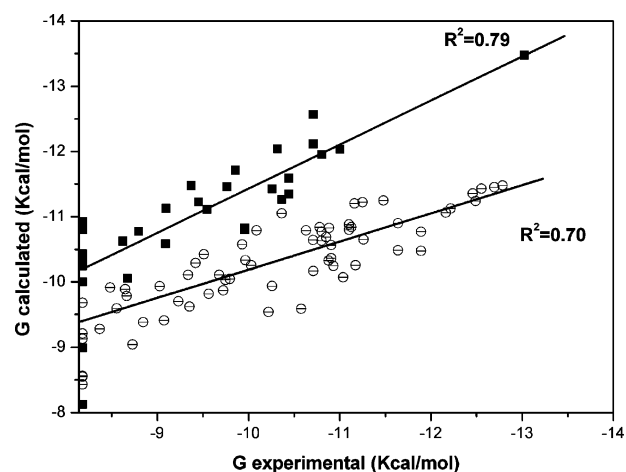


Figure 8. Plot of the experimental binding energy versus the average estimated binding free energy of the chosen cluster. Ligands with a morpholinic group are indicated by ■, while all the others are indicated by ○. The quadratic correlations, R² were calculated only for the ligands possessing a CB2 affinity greater than 1000 nM.

Binding Free Energy Estimation. Figure 8 reports the plot of experimental binding energy versus the average estimated binding free energy of the chosen cluster (see Experi-

mental Section) obtained by using the scoring function of AUTODOCK. The value of the quadratic correlation is very low ($R^2 = 0.31$); however, we observed that the plot splits the ligands into two different groups. Analyzing the structural characteristics of the compounds belonging to the two groups, we observed that the overestimated one was composed of all the ligands that had the morpholinic substituent.

Considering the plot constituted by two different groups and calculating the two quadratic correlations, we obtained a value of 0.79 for the morpholinic derivatives and a value of 0.70 for all the other ligands. Moreover, the predictive power of the model was tested by leave-one-out (LOO) cross-validation method,³⁷ where compounds are deleted one after another and prediction of the activity of the deleted compound is based on the QSAR model. This analysis showed a good predictive internal ability for both morpholinic derivatives ($q^2 = 0.74$) and the other ligands ($q^2 = 0.69$).

As the scoring function of AUTODOCK makes use of an empirical approach, and the free energy function is based on the principles of QSAR (quantitative structure–activity relationships) and was parametrized using a large number of protein–inhibitor complexes for which both structure and inhibition constants were known, the split of the ligands into two groups might be due to an overestimation of the AUTODOCK scoring function for the interaction between the morpholinic substituent and our CB2 model.

To verify if our CB2 model was able to predict the activity of other ligands, we used the 1-pentyl-3-phenylacetylindoles recently published by Huffman et al.³⁸ as test set. Table 4 shows the 28 compounds tested, their experimental and predicted free energy of binding, and the calculated SDEP (standard deviation of errors of prediction).

The nine ligands with the best CB2 affinity show an ortho substituent on the aryl ring (**JWH-252**, **JWH-250**, **JWH-306**, **JWH-311**, **JWH-314**, **JWH-203**, **JWH-204**, **JWH-249**, and **JWH-305**). In our model the high affinity of these ligands could be explained by their interaction with T3.37(118), that for most of them consists of the formation of a H bond, since the displacement of the substituent in meta or para position determined the loss of this interaction.

Conclusions

We have constructed 3D models of the active conformation of the cannabinoid receptors CB1 and CB2 based on crystallized bovine rhodopsin (1F88). A model of WIN55212-2 complexed with both receptors is described by means of docking studies, and a comparison of the CB2 and CB1 binding sites showed that the CB2/CB1 selectivity is mainly determined by interaction with the residues S3.31 and F5.46 in the CB2. These residues, corresponding to G3.31 and V5.46 in the CB1, are not conserved, and site-directed mutagenesis suggests that they play an important role.^{18,30} These results suggested that the CB2/CB1 selectivity could be increased by the presence in the ligands of a lipophilic group able to interact in the CB2 with F5.46 and a group able to form a H bond with S3.31.

Using the AUTODOCK program, we docked several ligands into the CB2 model, and their disposition in the receptor confirmed our binding hypothesis. Moreover, the results obtained using this method showed a good correlation between the estimated free energy binding and the experimental binding data. To better verify the predictivity of our CB2 model, an external test set of 28 ligands was used, and the SDEP value obtained suggests that this model can be considered quite reliable and predictive.

The cannabinoid receptors are an interesting therapeutic target; in fact, many computational studies on these receptors have been recently published.^{39–42} Our studies may be very useful in the search for new compounds, and a large database virtual screening analysis using this cannabinoid receptor model is already in progress.

Experimental Sections

Amino Acid Numbering. To refer to specific amino acids sequences, the numbering system suggested by Ballesteros and Weinstein is used.⁴³ The most highly conserved residue in each transmembrane helix (TMH) is assigned a value of 0.50, and this number is preceded by the TMH number and followed in parentheses by the sequence number. The other residues in the helix are given a locant value relative to this.

Nomenclature of χ_1 Rotamer. For the χ_1 torsion angle we used the nomenclature describe by Shi et al.⁴⁴ When the heavy atom in the γ position is in a position opposite the backbone nitrogen, looking from the β -carbon to the α carbon, the χ_1 is said to be trans; from the same viewpoint, when the γ heavy atom is opposite the backbone carbon, the χ_1 is said to be gauche+.

Methods. The crystal structure of bovine rhodopsin was taken from the Protein Data Bank,⁴⁵ while all the primary sequences were obtained from the SWISS-PROT protein sequence database.⁴⁶

As the function of the loops has still not been definite, like other authors^{47–49} we modeled only the TM domains of the two receptors. Furthermore, site-directed mutagenesis shows that the perturbation of the first extracellular loop does not affect the binding of WIN55212-2,⁵⁰ and in the second extracellular loop, only the mutation of two cysteines determines the loss of binding of the ligand, but the authors hypothesized that the mutation of these conserved residues resulted in an important structural perturbation, perhaps the elimination of a disulfide bridge.⁵¹

The sequential alignment of rhodopsin and the human cannabinoid receptors CB1 and CB2 was performed by means of CLUSTAL W,²⁰ using the Blosum series as a matrix, with a gap open penalty of 10 and a gap extension penalty of 0.05. The Psipred program^{21,22} was used in order to verify the presence of α -helices in our TM sequence hypothesis. Our results were in a perfect agreement with Salo et al.²³ who had taken into consideration several TM receptor sequences for alignment.

All the molecular mechanics and molecular dynamics calculations were performed by means of the MACROMODEL program⁵² by using the AMBER Force field. The electrostatic charges were those included in the force field and a distance-dependent dielectric constant of 4.0 was used. In molecular mechanics calculations (MM) the minimization algorithms were Steepest Descent followed by Conjugated Gradient until a convergence value of 0.05 kcal/Å³·mol; in molecular dynamics simulations the temperature was set at 300 K and the time step was 1 fs. All graphic manipulations and visualizations were performed by means of the Maestro⁵² and WebLabViewer programs,⁵³ while the quantum mechanical calculations were carried out using the Gaussian03 program.⁵⁴ The backbone conformation of the resulting protein structures was evaluated by inspection of the Psi/Phi Ramachandran plot obtained from PROCHECK analysis,²⁹ whereas ligand docking was performed using AUTODOCK 3.0.¹⁹

Construction of the Activated CB1 and CB2 Receptors. The 3D X-ray crystallographic structure of bovine rhodopsin registered in the Protein Data Bank was used as a direct template to construct the 7-TM helical structure of the CB1 and CB2 receptors by means of the Maestro program, on the basis of the alignment obtained from CLUSTAL W and Psipred analysis. Each model helix was capped with an acetyl group at the N-terminus and with an *N*-methyl group at the C-terminus. Each TM was subjected to preliminary minimization followed by 200 ps of MD, using a constraint of 50 kcal/mol on the C α and on the intra-helix H bonds. The final structures were then minimized using the same constraint. The receptor was reassembled on the basis of the rhodopsin structure rotating TM5

by 180° to let W5.43 and V/F5.46 turn toward the intra-helical channel.¹⁶ The whole system was then subjected to preliminary minimization followed by 400 ps of MD, using a constraint of 20 kcal/mol on the C α and a constraint with a decreasing force constant (10 to 0.1 kcal/mol) on the intra-helix H bonds.

The activated states of CB1 and CB2 were created by modification of the rhodopsin-based models thus obtained, by rotating TM3 and TM6 in a counterclockwise direction (extracellular point of view), straightening TM6, and adjusting the conformation of the χ_1 rotamer of W6.48 and F3.36 to trans and gauche+, respectively. The modified TM6 was optimized with the procedure used above for single TMs, and then the whole model was subjected to preliminary minimization, followed by 400 ps of MD, using a constraint of 20 kcal/mol on the C α and finally a minimization was applied to the structure obtained as the average of the last 100 ps.

Docking of AEA. The ligand was submitted to a conformational search of 1000 steps with an energy window for saving structure of 10 kJ/mol. The algorithm used was the Monte Carlo method with MMFFs as the force field and a distance-dependent dielectric constant of 1.0. The ligand was then minimized using the Conjugated Gradient method until a convergence value of 0.05 kcal/Å \cdot mol, using the same force field and dielectric constant used for the conformational search. Then the ligand was docked into both receptors using the AUTODOCK 3.0 program.¹⁹ The regions of interest used by AUTODOCK were defined by considering T3.33 as the central residue of a grid of 56, 46, and 50 points in the x, y, and z directions. A grid spacing of 0.375 Å and a distance-dependent function of the dielectric constant were used for the energetic map calculations.

Using the Lamarckian Genetic Algorithm, the compound was subjected to 250 runs of the AUTODOCK search, in which the default values of the other parameters were used. Cluster analysis was performed on the docked results using an RMS tolerance of 1.0 Å.

Docking of WIN55212-2. The ligand was submitted to a conformational search using the same parameters described above. For WIN55212-2, the best conformation was an s-trans geometry, in agreement with Reggio et al.⁵⁵ The atomic charges of the ligand were calculated by using the RESP method with the 6-31G* wave function on a structure previously minimized at the AM1 level.

WIN55212-2 was docked into both receptors through 400 ps of MD applying a constraint of 20 kcal/mol on the C α . Furthermore we applied a constraint on the main ligand–receptor interactions with a decreasing force constant (10, 5, 1 kcal/mol) on the first 300 ps of MD, leaving the ligand free in the last 100 steps. Finally a minimization was applied to the structure obtained as the average of the last 100 ps.

Analysis of Naphthyridine Derivative Geometry. To measure the strength of the intramolecular H bond, we used a method similar to the one employed by Cuma and co-workers.⁵⁶

We optimized models a and b of Table 5, using the B3LYP chemical model⁵⁷ with a 6-31G+* basis set; Regarding the optimization of model b, we used a constraint on the torsion involved in the H bond in order to prevent the formation of the H bond during optimization. The energy difference between the two optimized systems was about 30 kcal/mol, and this value gives us an idea of the high strength of this interaction.

Docking of the Ligands. Three representative ligands (**3a**, **JWH007**, **9**) were submitted to a conformational search using the same method described for AEA, and the best conformation was used as a general scaffold for the construction of the initial geometry of all the compounds; in all cases, the initial geometries thus obtained were then minimized.

Automated docking was carried out by means of the program AUTODOCK 3.0;¹⁹ AUTODOCK TOOLS⁵⁸ was used to identify the torsion angles in the ligands, add the solvent model, and assign partial atomic charges (Gasteiger for the ligands and Kollman for the receptors). The regions of interest used by AUTODOCK were defined by considering WIN55212-2 docked into the CB2 receptor as the central group; in particular, a grid of 54, 50, and 52 points

in the x, y, and z directions was constructed centered on the center of the mass of WIN55212-2. A grid spacing of 0.375 Å and a distance-dependent function of the dielectric constant were used for the energetic map calculations.

Using the Lamarckian Genetic Algorithm, all docked compounds were subjected to 100 runs of the AUTODOCK search, in which the default values of the other parameters were used. Cluster analysis was performed on the docked results using an RMS tolerance of 1.0 Å.

As we considered the WIN55212-2 binding geometry to be the one able to stabilize the active form of the CB2 receptor, the selection of the right cluster for each ligand docked was performed mainly on a geometrical basis, i.e., by choosing the best cluster among those in which the ligand had a binding geometry similar to that of WIN55212-2; namely, the one with a substituent inserted between TM3 and TM4 and another substituent directed toward the intracellular side of the receptor.

Regarding the most active compounds (those with a K_i lower than 1000 nM), it was found that for 85% of them the chosen cluster was also the one with the best average of estimated free energy, while for 6% of them the chosen cluster was the best populated one. For ligands **16**, **25b**, **JWH241**, **JWH236**, **JWH079**, **JWH261** and **JWH266** (9%), the chosen cluster did not belong to either of these two types (see Table 3) since neither the cluster with the best average of estimated free energy, or the best populated one possessed a binding geometry similar to that of WIN55212-2.

Regarding the ligands that showed a K_i higher than 1000 nM, the chosen cluster for 25% of them was the one possessing the best average of estimated free energy and for 12.5% the best populated one, whereas for 37.5% the chosen cluster did not belong to either of these two types; finally, for four ligands (25%) there were no clusters with a binding geometry similar to that of WIN55212-2, and therefore the cluster with the best average of estimated free energy was chosen.

References

- Gaoni, Y.; Mechoulam R. Isolation, structure, and partial synthesis of an active constituent of hashish. *J. Am. Chem. Soc.* **1964**, *86*, 1646–16477.
- Mechoulam, R.; Ben-Shabat, S. From gan-zi-gun-nu to anandamide and 2-arachidonoylglycerol: the ongoing story of cannabis. *Nat. Prod. Rev.* **1999**, *16*, 131–143.
- Breivogel, C. S.; Griffin, G.; Di Marzo, V.; Martin, B. R. *Mol. Pharmacol.* **2001**, *60*, 155–163.
- Matsuda, L. A.; Lolait, S. J.; Brownstein, M. J.; Young, A. C.; Bonner, T. I. Structure of a cannabinoid receptor and functional expression of the cloned cDNA. *Nature* **1990**, *346*, 561–564.
- Huffman, J. W.; Lainton, J. A. H. Recent developments in the medicinal chemistry of cannabinoids. *Curr. Med. Chem.* **1996**, *3*, 101–116.
- Herkenham, M.; Lynn, A. B.; Little, M. D.; Johnson, M. R.; Melvin, L. S.; De Costa, D. R.; Rice, K. C. Cannabinoid receptor localization in brain. *Proc. Natl. Acad. Sci. U.S.A.* **1990**, *87*, 1932–1936.
- Pertwee, R. G. Pharmacology of cannabinoid receptor ligands. *Curr. Med. Chem.* **1999**, *6*, 635–664.
- Galiegue, S.; Mary, S.; Marchand, J.; Dussossoy, D.; Carriere, D.; Carayon, P.; Bouaboula, M.; Shire, D.; Le Fur, G.; Casellas, P. Expression of central and peripheral cannabinoid receptors in human immune tissues and leukocyte subpopulations. *Eur. J. Biochem.* **1995**, *232*, 54–61.
- Recht, L. D.; Salmensen, R.; Rosetti, R.; Jang, T.; Pipia, G.; Kubiawski, T.; Karim, P.; Ross, A. H.; Zurier, R.; Litofsky, N. S.; Burstein S. Antitumor effects of ajulemic acid (CT3), a synthetic nonpsychoactive cannabinoid. *Biochem. Pharmacol.* **2001**, *62*, 755–763.
- Felder, C. C.; Joyce, K. E.; Briley, E. M.; Mansouri, J.; Mackie, K.; Blond, O.; Lai, Y.; Ma, A. L.; Mitchell R. L. Comparison of the pharmacology and signal transduction of the human cannabinoid CB1 and CB2 receptors. *Mol. Pharmacol.* **1995**, *48*, 443–450.
- Reggio, P. H. Pharmacophores for ligand recognition and activation/inactivation of the cannabinoid receptors. *Curr. Pharm. Des.* **2003**, *9*, 1607–1633.
- Colquhoun D. Binding, gating, affinity and efficacy: the interpretation of structure–activity relationships for agonists and of the effects of mutating receptors. *Br. J. Pharmacol.* **1998**, *125*, 924–947.

- (13) Gether U. Uncovering molecular mechanisms involved in activation of G protein-coupled receptors. *Endocr. Rev.* **2000**, *21*, 90–113.
- (14) Palczewski, K.; Kumasaka, T.; Hori, T.; Behnke, C. A.; Motoshima, H.; Fox, B. A.; Le Trong, I.; Teller, D. C.; Okada, T.; Stenkamp, R. E.; Yamamoto, M.; Miyano, M. Crystal structure of rhodopsin: A G protein-coupled receptor. *Science* **2000**, *289*, 739–745.
- (15) Reggio, P. H. Ligand-ligand and ligand-receptor approaches to modeling the cannabinoid CB1 and CB2 receptors: achievements and challenges. *Curr. Med. Chem.* **1999**, *6*, 665–683.
- (16) Song, Z. H.; Bonner, T. I. A lysine residue of the cannabinoid receptor is critical for receptor recognition by several agonists but not WIN55212-2. *Mol. Pharmacol.* **1996**, *49*, 891–896.
- (17) McAllister, S. D.; Rizvi, G.; Anavi-Goffer, S.; Hurst, D. P.; Barnett-Norris, J.; Lynch, D. L.; Reggio, P. H.; Abood, M. E. An aromatic microdomain at the cannabinoid CB1 receptor constitutes an agonist/inverse agonist binding region. *J. Med. Chem.* **2003**, *46*, 5139–5152.
- (18) Song, Z. H.; Slowey, C. A.; Hurst, D. P.; Reggio, P. H. The difference between the CB1 and CB2 cannabinoid receptors at position 5.46 is crucial for the selectivity of WIN55212-2 for CB2. *Mol. Pharmacol.* **1999**, *56*, 834–840.
- (19) Morris, G. M.; Goodsell, D. S.; Halliday, R. S.; Huey, R.; Hart, W. E.; Belew, R. K.; Olson, A. J. Automated docking using a Lamarckian genetic algorithm and empirical binding free energy function. *J. Comput. Chem.* **1998**, *19*, 1639–1662.
- (20) Thompson, J. D.; Higgins, D. G.; Gibson, T. J. CLUSTAL W: improving the sensitivity of progressive multiple sequence alignment through sequence weighting, position-specific gap penalties and weight matrix choice. *Nucleic Acids Res.* **1994**, *22*, 4673–4680.
- (21) McGuffin, L. J.; Bryson, K.; Jones, D. T. The PSIPRED protein structure prediction server. *Bioinformatics* **2000**, *16*, 404–405.
- (22) Jones, D. T.; Protein secondary structure prediction based on position-specific scoring matrices. *J. Mol. Biol.* **1999**, *292*, 195–202.
- (23) Salo, O. M.; Lahtela-Kakkonen, M.; Gynther, J.; Jarvinen, T.; Poso, A. Development of a 3D model for the human cannabinoid CB1 receptor. *J. Med. Chem.* **2004**, *47*, 3048–3057.
- (24) Ballesteros, J. A.; Jensen, A. D.; Liapakis, G.; Rasmussen, S. G.; Shi, L.; Gether, U.; Javitch, J. A. Activation of the beta 2-adrenergic receptor involves disruption of an ionic lock between the cytoplasmic ends of transmembrane segments 3 and 6. *J. Biol. Chem.* **2001**, *276*, 29171–29177.
- (25) Sansom, M. S.; Weinstein, H. Hinges, swivels and switches: the role of prolines in signalling via transmembrane alpha-helices. *Trends Pharmacol. Sci.* **2000**, *21*, 445–451.
- (26) Jensen, A. D.; Guarnieri, F.; Rasmussen, S. G.; Asmar, F.; Ballesteros, J. A.; Gether, U. Agonist-induced conformational changes at the cytoplasmic side of transmembrane segment 6 in the beta 2 adrenergic receptor mapped by site-selective fluorescent labeling. *J. Biol. Chem.* **2001**, *276*, 9279–9290.
- (27) Shi, L.; Liapakis, G.; Xu, R.; Guarnieri, F.; Ballesteros, J. A.; Javitch, J. A. Beta2 adrenergic receptor activation. Modulation of the proline kink in transmembrane 6 by a rotamer toggle switch. *J. Biol. Chem.* **2002**, *277*, 40989–40996.
- (28) Singh, R.; Hurst, D. P.; Barnett-Norris, J.; Lynch, D. L.; Reggio, P. H.; Guarnieri, F. Activation of the cannabinoid CB1 receptor may involve a W6.48/F3.36 rotamer toggle switch. *J. Pept. Res.* **2002**, *60*, 357–370.
- (29) Laskowski, R. A.; MacArthur, M. W.; Moss, D. S.; Thornton, J. M. PROCHECK: a program to check the stereochemical quality of protein structures. *J. Appl. Crystallogr.* **1993**, *26*, 283–291.
- (30) Tao, Q.; McAllister, S. D.; Andreassi, J.; Nowell, K. W.; Cabral, G. A.; Hurst, D. P.; Bachtel, K.; Ekman, M. C.; Reggio, P. H.; Abood, M. E. Role of a conserved lysine residue in the peripheral cannabinoid receptor (CB2): evidence for subtype specificity. *Mol. Pharmacol.* **1999**, *55*, 605–613.
- (31) GRID v. 22 Molecular Discovery Ltd. (<http://www.moldiscovery.com>).
- (32) Huffman, J. W.; Zengin, G.; Wu, M. J.; Lu, J.; Hynd, G.; Bushell, K.; Thompson, A. L.; Bushell, S.; Tartal, C.; Hurst, D. P.; Reggio, P. H.; Selley, D. E.; Cassidy, M. P.; Wiley, J. L.; Martin, B. R. Structure-activity relationships for 1-alkyl-3-(1-naphthyl)indoles at the cannabinoid CB1 and CB2 receptors: steric and electronic effects of naphthoyl substituents. New highly selective CB2 receptor agonists. *Bioorg. Med. Chem.* **2005**, *13*, 89–112.
- (33) Vannacci, A.; Giannini, L.; Passani, M. B.; Di Felice, A.; Pierpaoli, S.; Zagli, G.; Fantappiè, O.; Mazzanti, R.; Masini, E.; Mannaioni, P. F. The endocannabinoid 2-Arachidonylglycerol decreases the immunological activation of guinea pig mast cells: involvement of nitric oxide and eicosanoids. *J. Pharmacol. Exp. Ther.* **2004**, *311*, 256–264.
- (34) Unpublished results from our laboratory.
- (35) Ferrarini, P. L.; Calderone, V.; Cavallini, T.; Manera, C.; Saccomanni, G.; Pani, L.; Ruiu, S.; Gessa, G. L. Synthesis and biological evaluation of 1,8-naphthyridin-4(1H)-on-3-carboxamide derivatives as new ligands of cannabinoid receptors. *Bioorg. Med. Chem.* **2004**, *12*, 1921–1933.
- (36) Gallant, M.; Dufresne, C.; Gareau, Y.; Guay, D.; Leblanc, Y.; Prasad, P.; Rochette, C.; Sawyer, N.; Slipetz, D. M.; Tremblay, N.; Metters, K. M.; Labelle, M. New class of potent ligands for the human peripheral cannabinoid receptor. *Bioorg. Med. Chem. Lett.* **1996**, *6*, 2263–2268.
- (37) Chatterjee, S.; Hadi, A. S.; Price, B. *Regression Analysis of Examples*; John Wiley & Sons: New York, 2000.
- (38) Huffman, J. W.; Szklennik, P. V.; Almond, A.; Bushell, K.; Selley, D. E.; He, H.; Cassidy, M. P.; Wiley, J. L.; Martin, B. R. 1-Pentyl-3-phenylacetylindoles, a new class of cannabinimetic indoles. *Bioorg. Med. Chem. Lett.* **2005**, *15*, 4110–4113.
- (39) Montero, C.; Campillo, N. E.; Goya, P.; Páez, J. A. Homology models of the cannabinoid CB1 and CB2 receptors. A docking analysis study. *Eur. J. Med. Chem.* **2005**, *40*, 75–83.
- (40) Shim, J. Y.; Welsh, W. J.; Howlett, A. C. Homology model of the CB1 cannabinoid receptor: sites critical for nonclassical cannabinoid agonist interaction. *Biopolymers* **2003**, *71*, 169–189.
- (41) Xie, X. Q.; Chen, J. Z.; Billings, E. M. 3D structural model of the G-protein-coupled cannabinoid CB2 receptor. *Proteins* **2003**, *53*, 307–319.
- (42) Salo, O. M. H.; Raitio, K. H.; Savinainen, J. R.; Nevalainen, T.; Lahtela-Kakkonen, M.; Laitinen, J. T.; Jarvinen, T.; Poso, A. Virtual screening of novel CB2 ligands using a comparative model of the human cannabinoid CB2 receptor. *J. Med. Chem.* **2005**, *48*, 7166–7171.
- (43) Ballesteros, J. A.; Weinstein, H. W. Integrated methods for the construction of three-dimensional models and computational probing of structure-function relations in G-protein coupled receptors. *Methods Neurosci.* **1995**, *25*, 366–428.
- (44) Shi, L.; Liapakis, G.; Xu, R.; Guarnieri, F.; Ballesteros, J. A.; Javitch, J. A. β_2 Adrenergic receptor activation. *J. Biol. Chem.* **2002**, *277*, 40989–40996.
- (45) Berman, H. M.; Westbrook, J.; Feng, Z.; Gilliland, G.; Bhat, T. N.; Weissig, H.; Shindyalov, I. N.; Bourne, P. E. The Protein Data Bank. *Nucl. Acids Res.* **2000**, *28*, 235–242.
- (46) Gasteiger, E.; Gattiker, A.; Hoogland, C.; Ivanyi, I.; Appel, R. D.; Bairoch, A. ExPASy: the proteomics server for in-depth protein knowledge and analysis. *Nucleic Acids Res.* **2003**, *31*, 3784–3788.
- (47) Bramblett, R. D.; Panu, A. M.; Ballesteros, J. A.; Reggio, P. H. Construction of a 3D model of the cannabinoid CB1 receptor: determination of helix ends and helix orientation. *Life Sci.* **1995**, *56*, 1971–1982.
- (48) McAllister, S. D.; Tao, Q.; Barnett-Norris, J.; Buehner, K.; Hurst, D. P.; Guarnieri, F.; Reggio, P. H.; Nowell, K. W.; Cabral, G. A.; Abood, M. E. A critical role for a tyrosine residue in the cannabinoid receptors for ligand recognition. *Biochem. Pharmacol.* **2002**, *63*, 2121–2136.
- (49) Barnett-Norris, J.; Hurst, D. P.; Lynch, D. L.; Guarnieri, F.; Makriyannis, A.; Reggio, P. H. Conformational memories and the endocannabinoid binding site at the cannabinoid CB1 receptor. *J. Med. Chem.* **2002**, *45*, 3649–3659.
- (50) Murphy, J. W.; Kendall, D. A. Integrity of extracellular loop 1 of the human cannabinoid receptor 1 is critical for high-affinity binding of the ligand CP55940 but not SR 141716A. *Biochem. Pharmacol.* **2003**, *65*, 1623–1631.
- (51) Gouldson, P.; Calandra, B.; Legoux, P.; Kernéis, A.; Rinaldi-Carmona, M.; Barth, F.; Le Fur, G.; Ferrara, P.; Shire, D. Mutational analysis and molecular modelling of the antagonist SR 144528 binding site on the human cannabinoid CB2 receptor. *Eur. J. Pharm.* **2000**, *401*, 17–25.
- (52) Macromodel ver. 8.5, Schrodinger Inc., 1999.
- (53) WebLab Viewer Pro 3.7 (Accelrys Inc., San Diego, CA).
- (54) Gaussian 03, Revision C.02, Frisch, M. J.; Trucks, G. W.; Schlegel, H. B.; Scuseria, G. E.; Robb, M. A.; Cheeseman, J. R.; Montgomery, Jr., J. A.; Vreven, T.; Kudin, K. N.; Burant, J. C.; Millam, J. M.; Iyengar, S. S.; Tomasi, J.; Barone, V.; Mennucci, B.; Cossi, M.; Scalmani, G.; Rega, N.; Petersson, G. A.; Nakatsuji, H.; Hada, M.; Ehara, M.; Toyota, K.; Fukuda, R.; Hasegawa, J.; Ishida, M.; Nakajima, T.; Honda, Y.; Kitao, O.; Nakai, H.; Klene, M.; Li, X.; Knox, J. E.; Hratchian, H. P.; Cross, J. B.; Bakken, V.; Adamo, C.; Jaramillo, J.; Gomperts, R.; Stratmann, R. E.; Yazyev, O.; Austin, A. J.; Cammi, R.; Pomelli, C.; Ochterski, J. W.; Ayala, P. Y.; Morokuma, K.; Voth, G. A.; Salvador, P.; Dannenberg, J. J.; Zakrzewski, V. G.; Dapprich, S.; Daniels, A. D.; Strain, M. C.; Farkas, O.; Malick, D. K.; Rabuck, A. D.; Raghavachari, K.;

- Foresman, J. B.; Ortiz, J. V.; Cui, Q.; Baboul, A. G.; Clifford, S.; Cioslowski, J.; Stefanov, B. B.; Liu, G.; Liashenko, A.; Piskorz, P.; Komaromi, I.; Martin, R. L.; Fox, D. J.; Keith, T.; Al-Laham, M. A.; Peng, C. Y.; Nanayakkara, A.; Challacombe, M.; Gill, P. M. W.; Johnson, B.; Chen, W.; Wong, M. W.; Gonzalez, C.; and Pople, J. A.; Gaussian, Inc., Wallingford, CT, 2004.
- (55) Reggio, P. H.; Basu-Dutt, S.; Barnett-Norris, J.; Castro, M. T.; Hurst, D. P.; Seltzman, H. H.; Roche, M. J.; Gilliam, A. F.; Thomas, B. F.; Stevenson, L. A.; Pertwee, R. G.; Abood, M. E. The bioactive conformation of aminoalkylindoles at the cannabinoid CB1 and CB2 receptors: insights gained from (E)- and (Z)-naphthylidene indenes. *J. Med. Chem.* **1998**, *41*, 5177–87.
- (56) Cuma, M.; Scheiner, S.; Kar, T. Effect of adjoining aromatic ring upon excited-state proton transfer, o-hydroxybenzaldehyde. *THEOCHEM* **1999**, *467*, 37–49.
- (57) Bauschlicher, C. W. A comparison of the accuracy of different functionals. *Chem. Phys. Lett.* **1995**, *246*, 40–44.
- (58) <http://www.scripps.edu/~sanner/python/adt>

JM050875U